A Joint Seismic and Geodynamic Study of Three-Dimensional Earth Structure and Thermal Convection in Earth's Mantle

Alessandro Forte
Centre GEOTOP
Montréal, Canada

1. Introduction

We will focus on the *dynamics of the mantle* and, in particular on how the internal dynamics are manifested at the Earth's surface. It is now generally accepted that an understanding of thermal convection in the mantle is necessary for explaining a multitude of geophysical and geological processes which we can observe and measure at the surface of the Earth, such as continental drift, earthquakes, mountain building, volcanism, perturbations in Earth's gravitational field, variations in oceanic bathymetry and continental elevation, and long-term changes in global sea-level variations, to name just a few.

The mathematical and numerical models which will be presented here are undoubtedly greatly simplified representations of the actual physical processes occurring deep inside our planet. We must therefore recognize the need for caution when using these models to investigate convection dynamics in the mantle. I expect, nonetheless, that the models we will develop here will allow us to grasp some of the essential aspects of the physics needed to understand mantle dynamics.

As noted above, geophysicists who wish to develop a physical understanding of dynamic processes deep inside our planet must first consider the implications and constraints provided by fundamental observations of processes occuring at the surface of our planet. Let us consider here a number of such observations which have played a historically important role.

The major sedimentary rock layers exposed in the Grand Canyon range in age from 200 million to about 2 billion years old. Most were deposited in shallow seas and near ancient sea shores. The average elevation is ~2200 m and the average elevation of the Colorado River is ~670 m (almost a mile below top).

1906 San Francisco Earthquake

5:12 AM - April 18, Magnitude = ~7.9

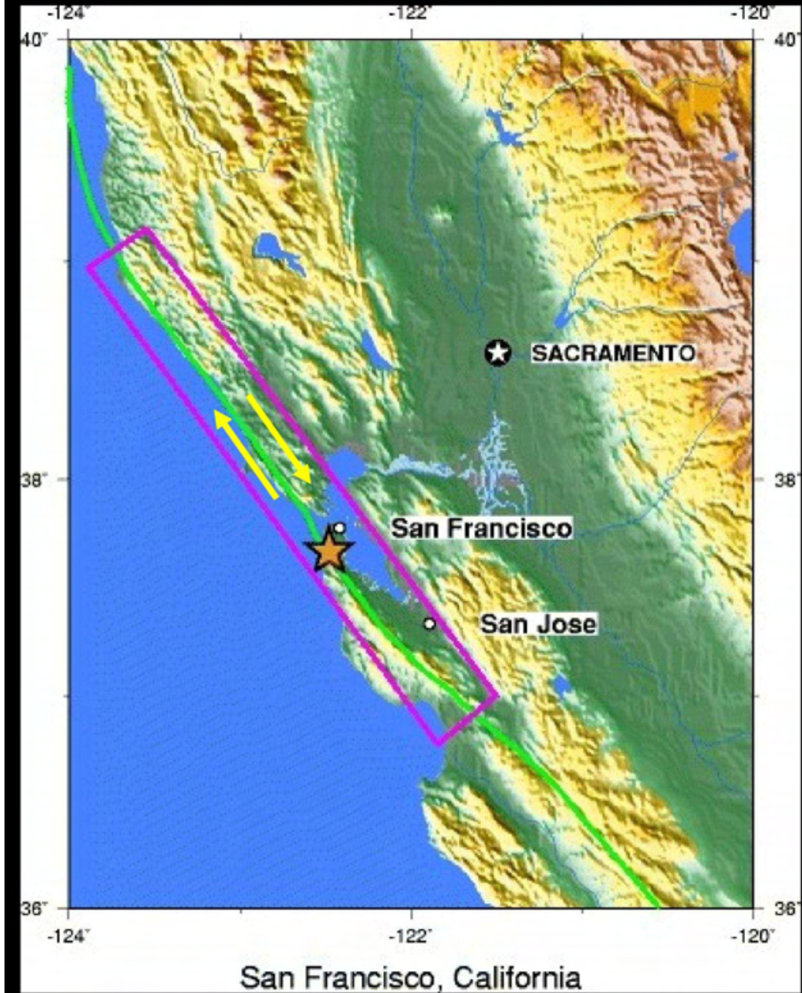

A 470 kilometre portion of the San Andreas fault (*green line*) slipped: slip ranged from 2.5 m in the south to 8 m in the north. (*Yellow arrows show sense of rupture.*)

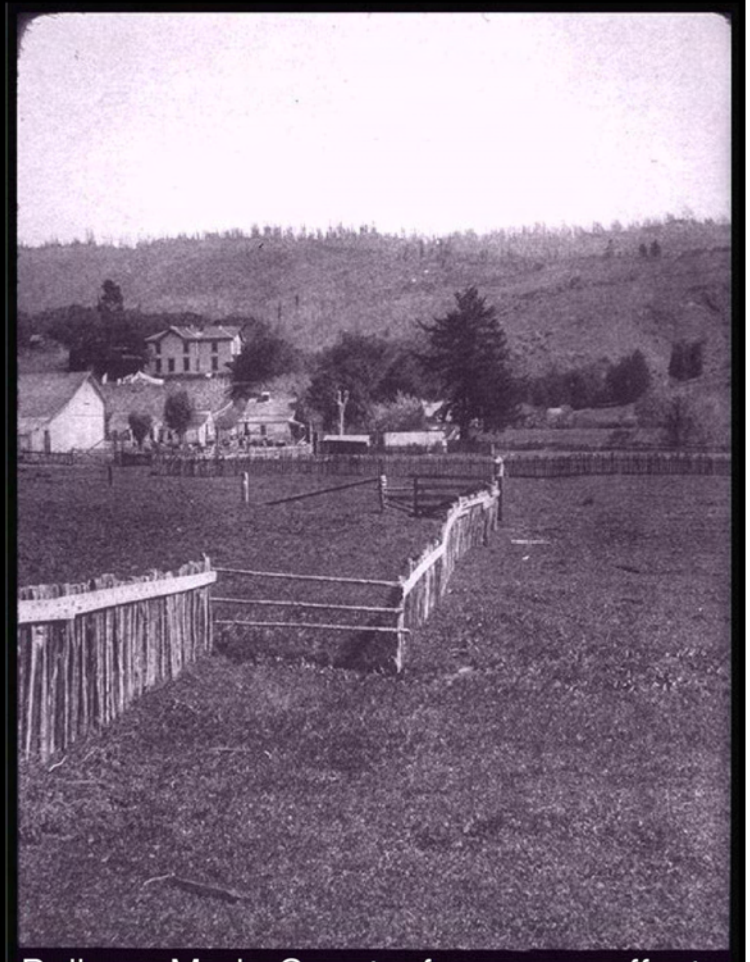

Bolinas, Marin County: fence was offset about 2.5 m along the trace of the fault. (*Looking northwest.*)

San Francisco 1906 - View down Market Street

Magnitude = ~7.9 (Radiated energy is equivalent to 790 A-bombs.)

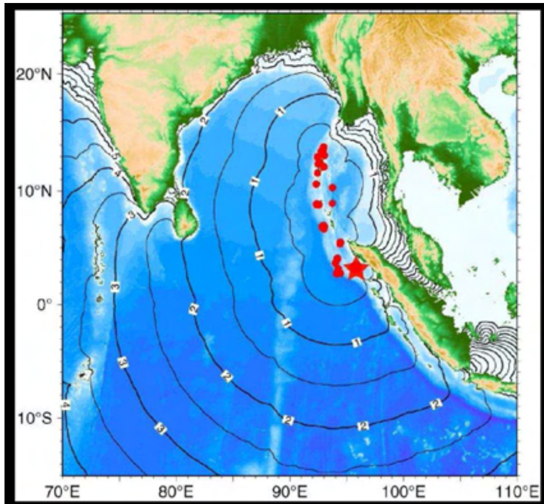

Sumatra Earthquake & Tsunami
26 Dec 2004, Magnitude = 9.0

(Radiated energy is equivalent to 25,000 A-bombs.)

Fourth largest earthquake in the world since 1900.

Banda-Aceh
(before Dec 26)

Banda-Aceh
(after Dec 26)

Continental Drift

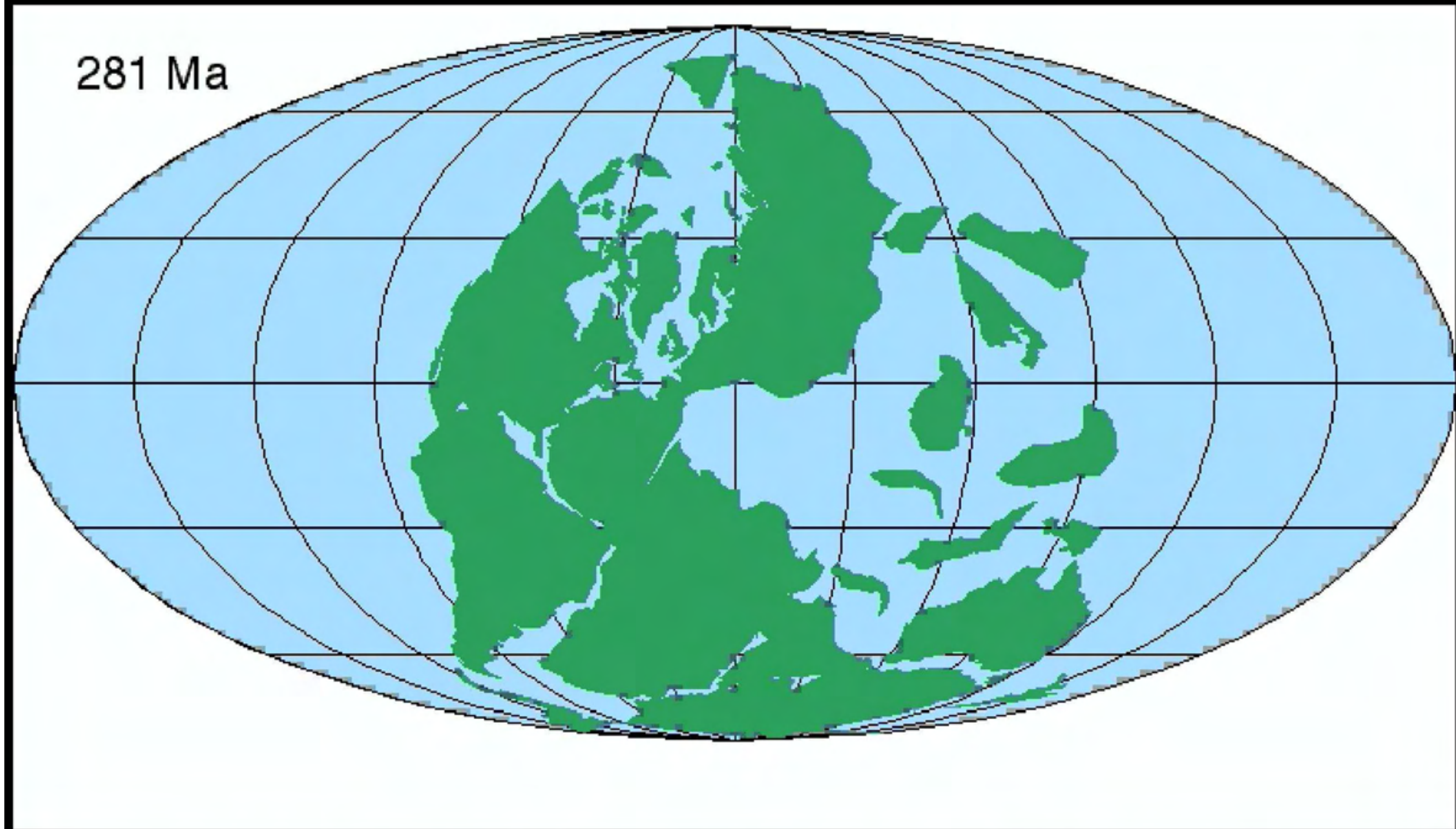

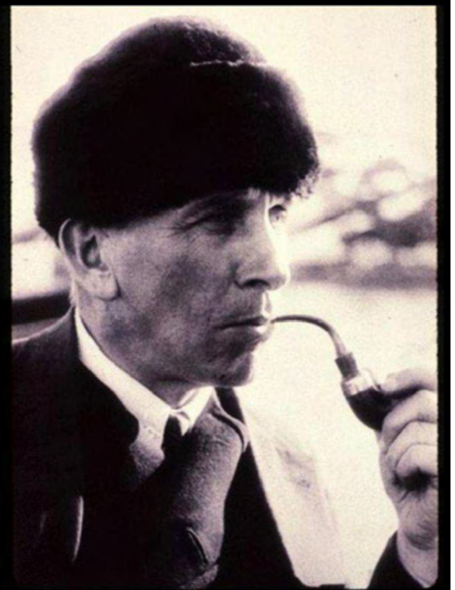

Alfred Wegener, 1915: "*The Origin of Continents and Oceans*"

Source: David Rowley - *The Paleogeographic Atlas Project* (University of Chicago)

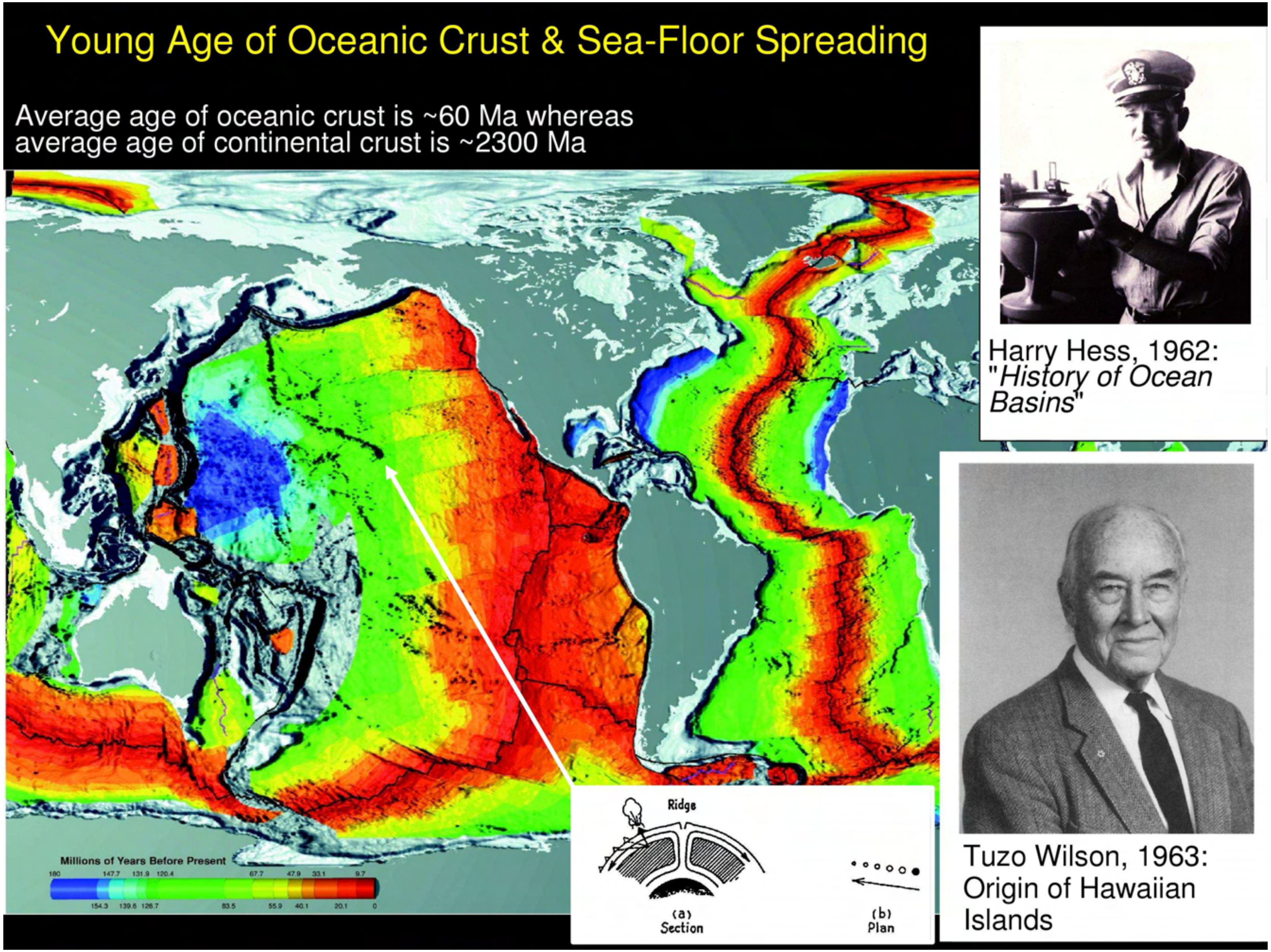
Young Age of Oceanic Crust & Sea-Floor Spreading
Average age of oceanic crust is ~60 Ma whereas
average age of continental crust is ~2300 Ma
Millions of Years Before Present
180 147.7 131.9 120.4 67.7 47.9 33.1 9.7
154.3 139.6 126.7 83.5 55.9 40.1 20.1 0
Ridge
(a)
Section
(b)
Plan
Harry Hess, 1962:
"*History of Ocean Basins*"
Tuzo Wilson, 1963:
Origin of Hawaiian Islands

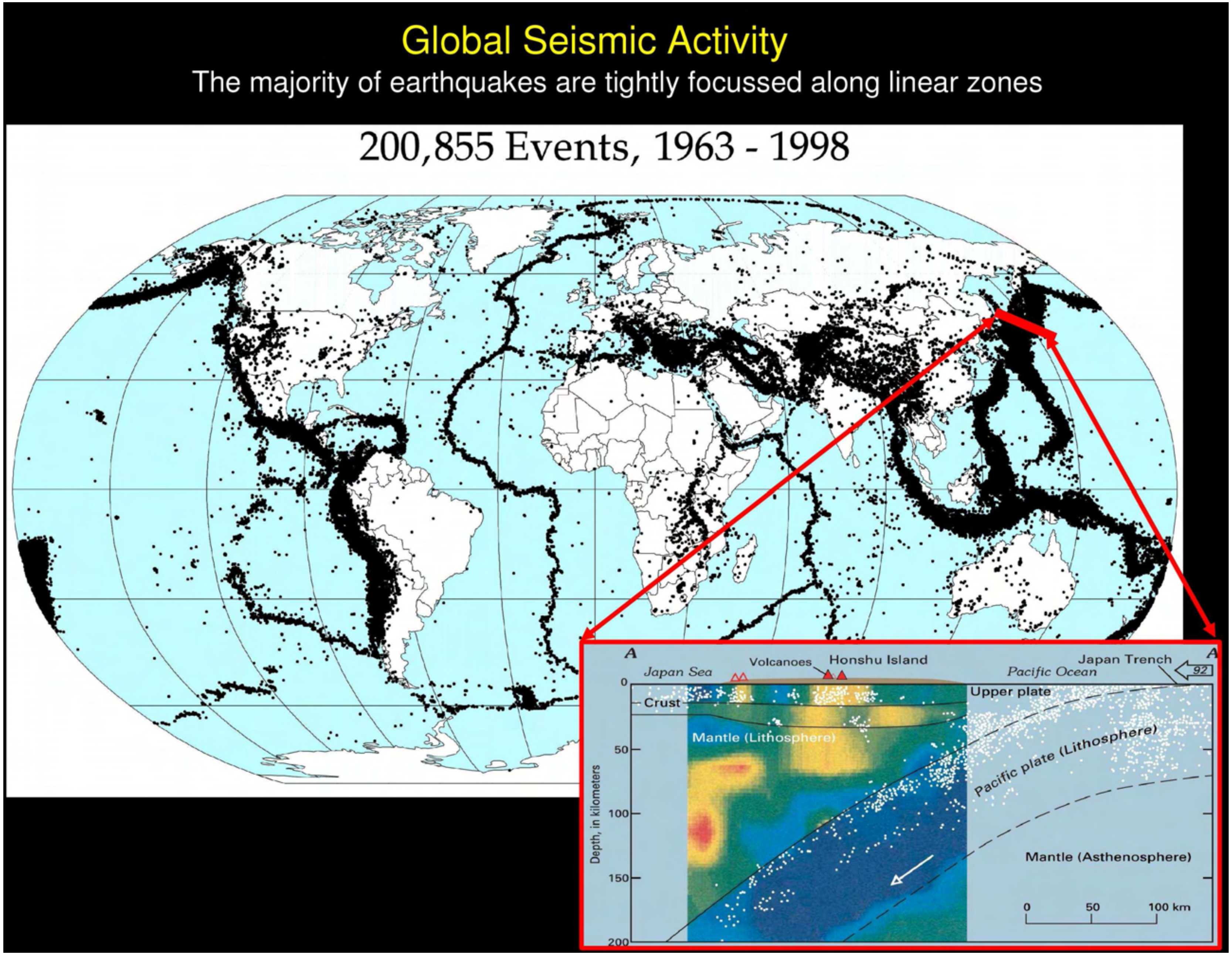
Global Seismic Activity
The majority of earthquakes are tightly focussed along linear zones
200,855 Events, 1963 - 1998
A
Japan Sea
Volcanoes
Honshu Island
Japan Trench
Pacific Ocean
A'
92
0
Crust
Upper plate
Mantle (Lithosphere)
50
Pacific plate (Lithosphere)
100
Depth, in kilometers
150
Mantle (Asthenosphere)
0
50
100 km
200

Plate Tectonics "Revolution"

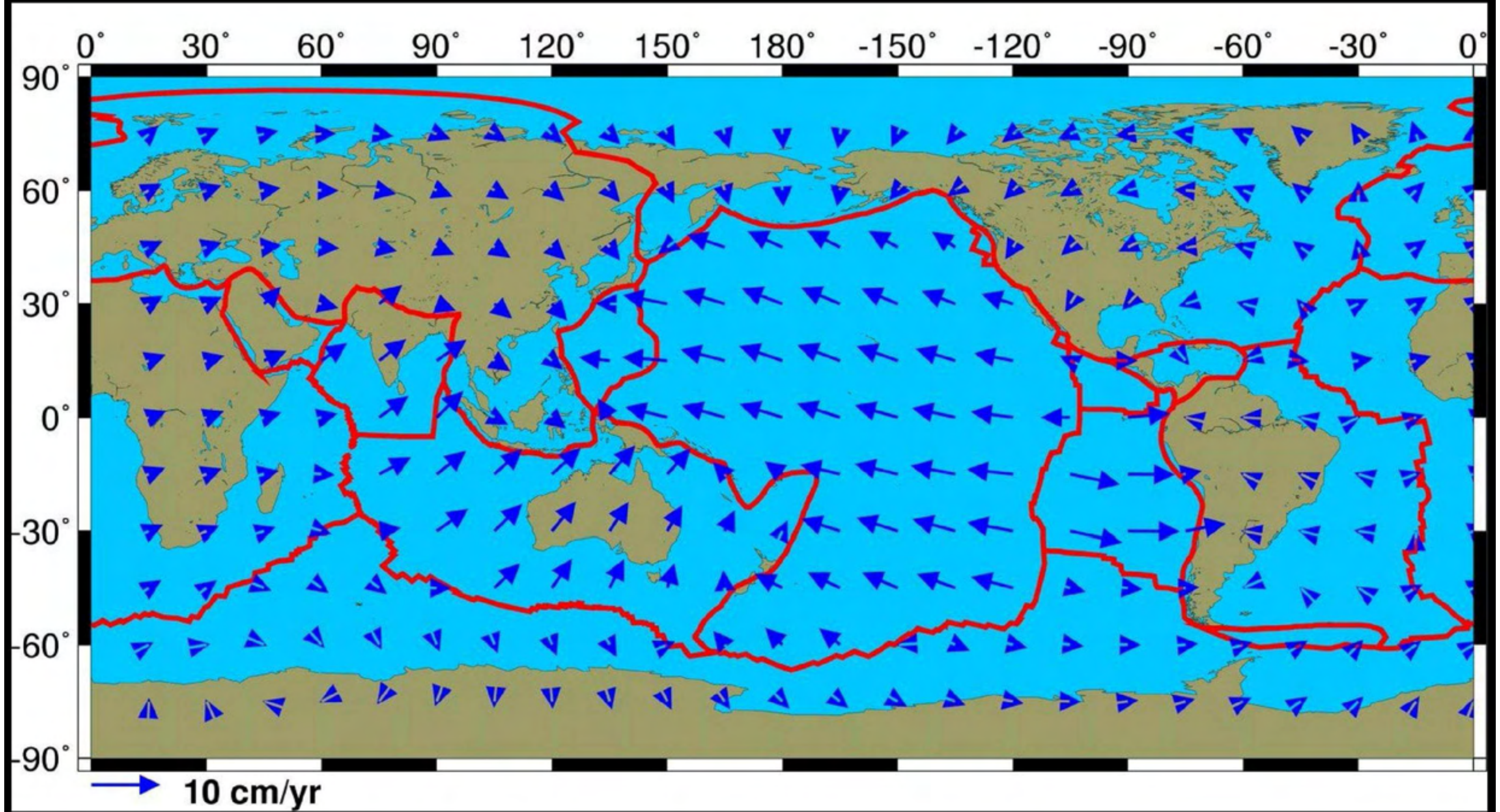

Earth's crust is divided into a small number of large, essentially rigid plates which move relative to each other. This theory provides a framework for understanding the connections between an assortment of surface processes such as continental drift, earthquakes, volcanism, mountain formation, and variations in ocean-floor bathymetry (the mid-ocean ridge system).

Plate tectonics has helped to understand the relationship between continental drift, sea-floor spreading, earthquakes and volcanism but it provides little insight into how the heat engine inside the mantle actually operates nor does it tell us anything about the flow patterns deep below the crust.

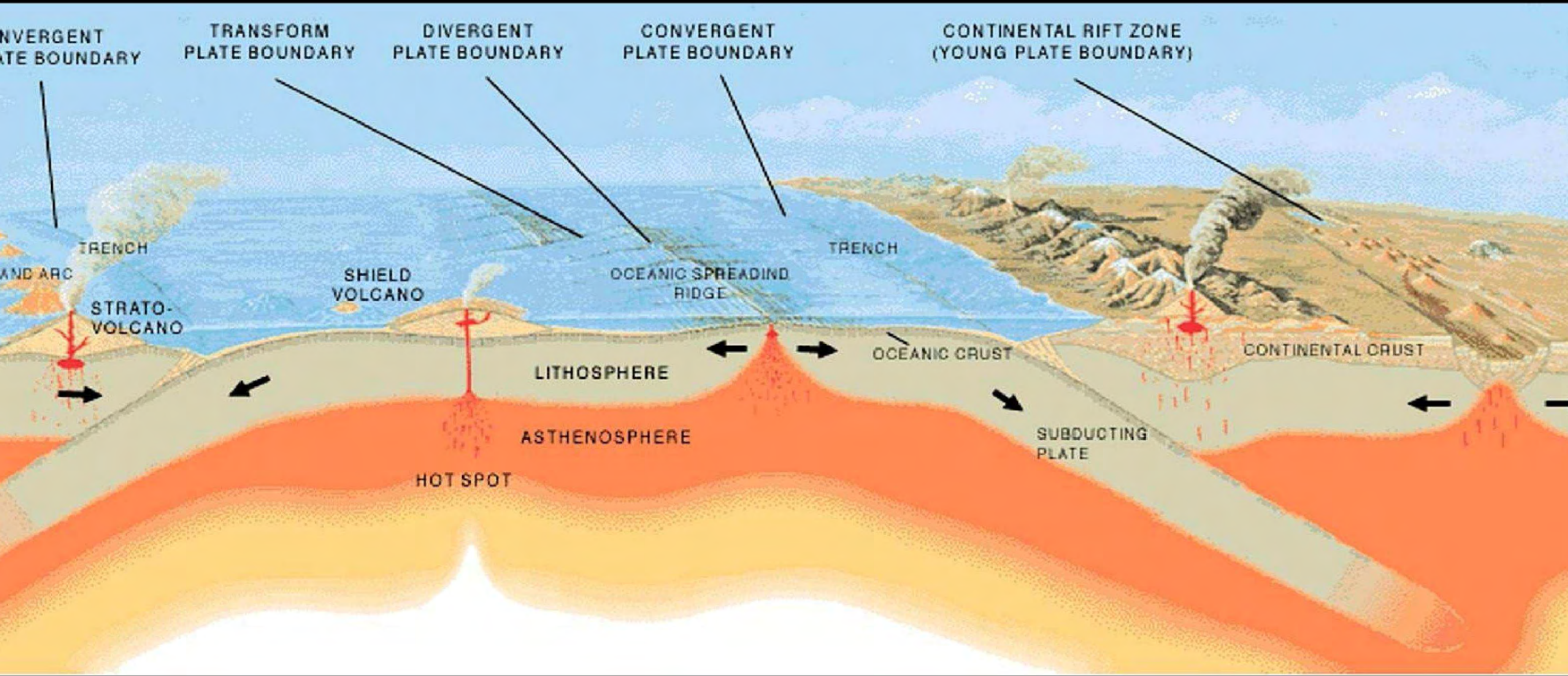

These different surface manifestations of the hidden dynamics in Earth’s interior have been very important in developing the Plate Tectonic hypothesis of how the Earth works, but they are fundamentally limited because they do not allow us to directly ’see’ into our planet’s interior. Seismology is by far the most important tool we have for mapping out the structure of Earth’s interior.

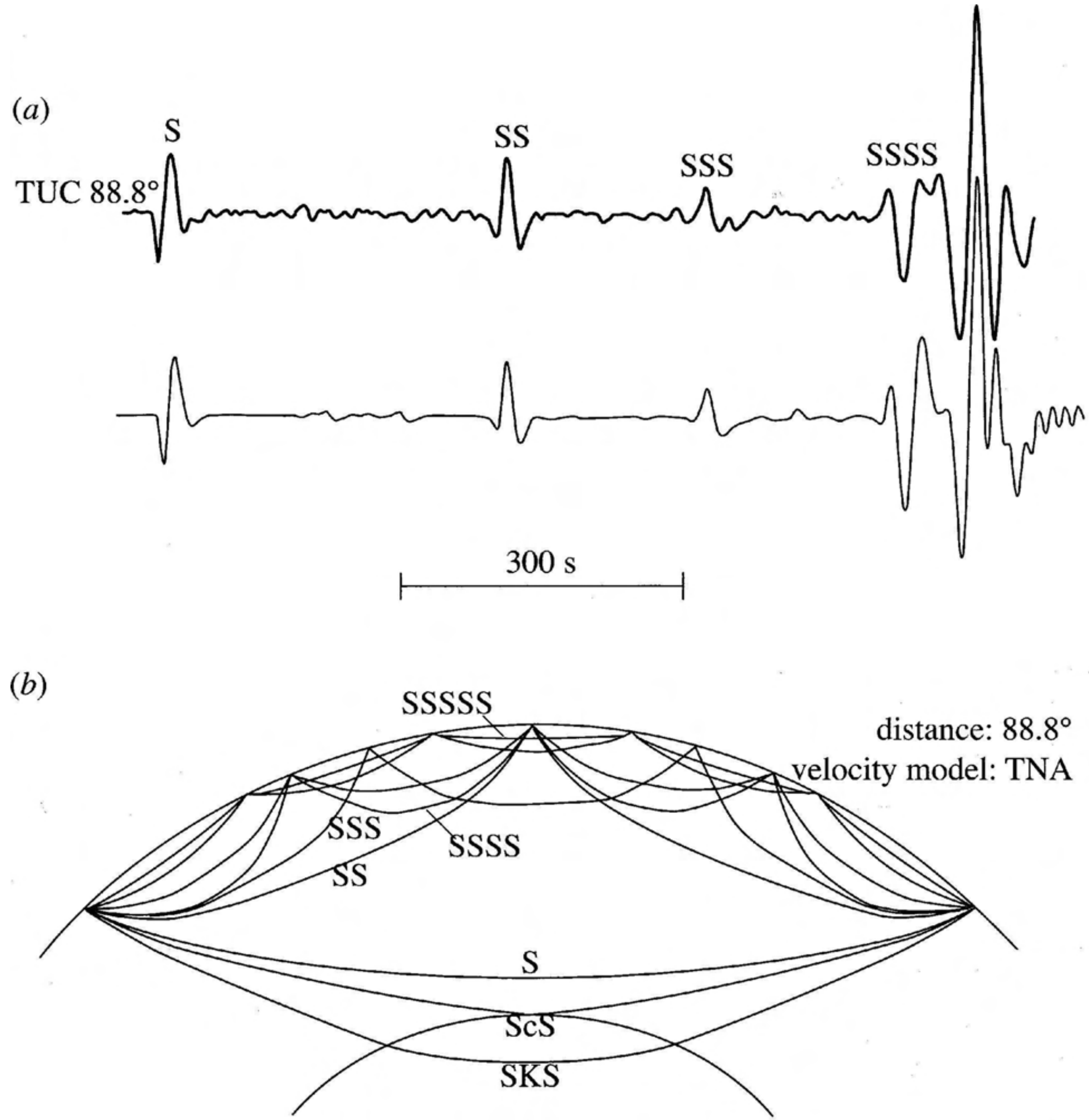

(a)
S
SS
SSS
SSSS
TUC 88.8°
300 s
(b)
SSSSS
distance: 88.8°
velocity model: TNA
SSS
SSSS
SS
S
ScS
SKS

By measuring and analyzing the travel times of seismic waves (as shown in the previous figure), seismologists have developed complete models of the 1-D depth dependent average structure of the Earth's interior which has been used to determine the increase in temperature and pressure from the surface of the Earth down to the centre of Earth's core (see next figure).

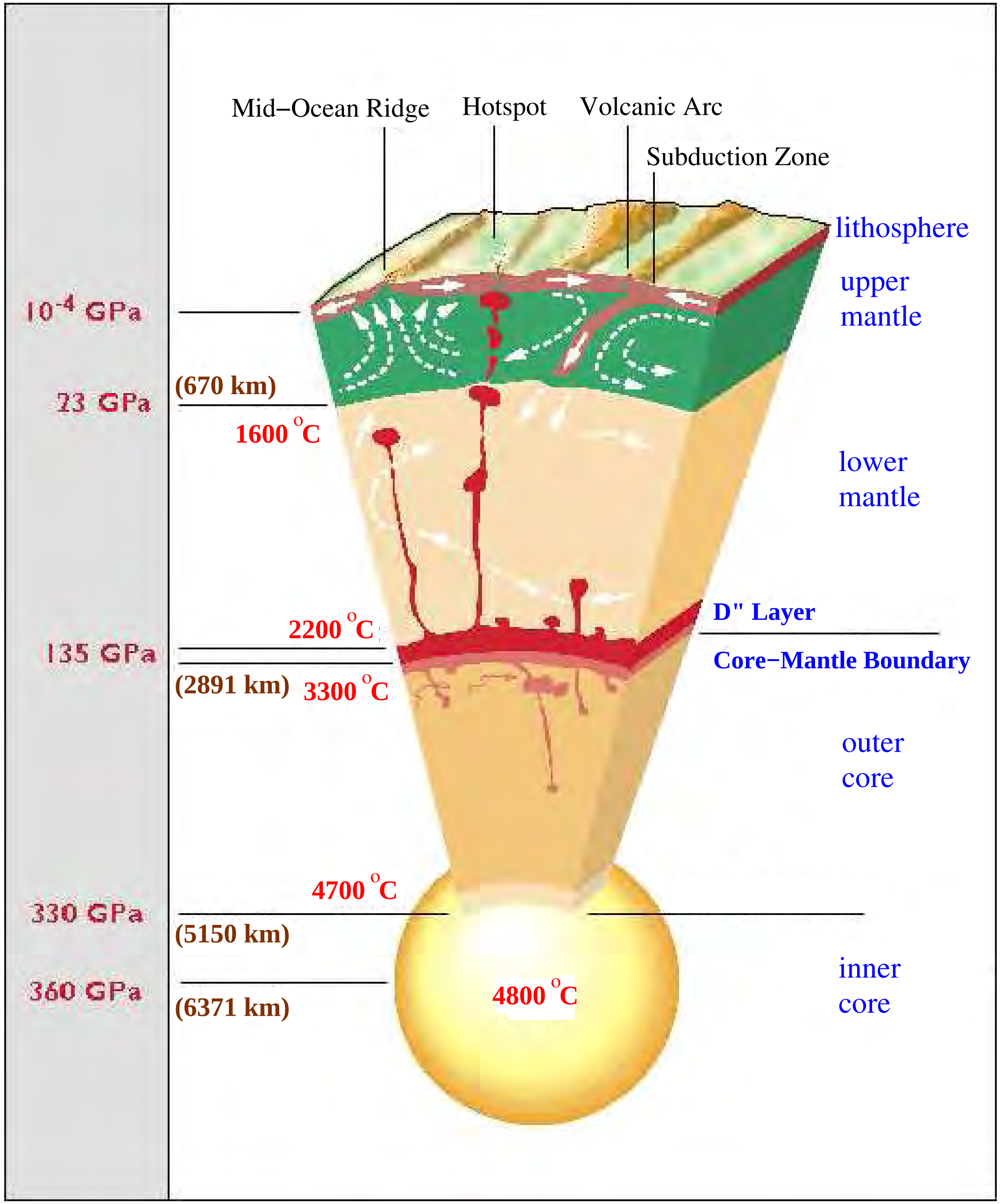

Fig. 1. Radial Earth structure and a geological conception of Earth's internal dynamics.
[adapted from *Besse & Courtillot*]

2. Rheological Properties of the Mantle: Viscosity

Plate tectonics clearly shows the ability of the mantle to creep or 'flow' over geological time scales. The physical possibility of this flow is due to the presence of natural *imperfections* in the crystalline structure of the minerals which constitute the rocks in the mantle. These imperfections are actually atomic-scale *defects* in the lattice of the crystal grains in minerals (*e.g., Nicolas & Poirier*, 1976; *Carter*, 1976; *Weertman*, 1978). If the ambient temperature is sufficiently high, the imposition of stresses on the rocks will cause the mineral defects to propagate and they thus permit mantle rocks to effectively 'flow'. The flow can persist for as long as the imposed stresses are maintained and thus mantle deformation can achieve a steady state rate.

The steady-state creep of mantle rocks may then be characterized by a single parameter called the *effective viscosity* (*e.g., Gordon*, 1965; *Weertman & Weertman*, 1975). A general formula for the effective viscosity of the mantle, which is based on the microphysical creep mechanisms described in the references cited above, is as follows:

$$\eta = A\, d^m\, \tau^{-n}\, \mathrm{k}T\, \exp\left[\frac{\Delta E + P\Delta V}{\mathrm{k}T}\right] \tag{1}$$

in which A is a dimensional constant which depends on the details of the creep processes, d is the effective *grain size* of the crystal grains, $\tau = \sqrt{\tau_{ij}\tau_{ij}}$ is the square root of the second invariant of the *deviatoric stress* field (*Stocker & Ashby*, 1973), k is Boltzmann's constant, T is the *absolute temperature*, ΔE is the creep *activation energy*, ΔV is the creep *activation volume*, and P is the total ambient *pressure*.

If mantle creep occurs primarily through the *diffusion* of point defects, the effective viscosity in expression (1) is independent of stress (*i.e.*, $n = 0$). For this *diffusion creep* the dependence on grain size is significant and generally m ranges from 2 to 3. An alternative mechanism for mantle creep involves the glide and climb of *dislocations*, in which case the effective viscosity in (1) will be independent of grain size (*i.e.*, $m = 0$) but will be sensitive to ambient deviatoric stress. For this *dislocation creep*, laboratory experiments on olivine or dunite suggest the stress exponent n will be near 3 (*e.g.*, *Post & Griggs*, 1973).

The theoretical expression (1) does not explicitly show the importance of *chemical* environment (*e.g.*, H_2O, CO_2) on mantle viscosity. Many studies have suggested a strong impact of chemistry on mantle creep (*e.g.*, *Ricoult & Kohlstedt*, 1985;

Karato et al. 1986; *Borch & Green*, 1987; *Hirth & Kohlstedt*, 2003).

The strong dependence of effective viscosity on temperature and pressure can be represented in terms of a *homologous temperature*, T/T_{melt}, as follows:

$$\eta = \eta_o \exp\left[g\,\frac{T_{melt}}{T}\right] \tag{2}$$

This dependence of viscosity on melting temperature, which has been observed in metallurgy, was extended to the crystalline rocks in the mantle by *Weertman* (1970) for the purpose of estimating viscosity in the deep mantle. The factor g in expression (2) is empirical, and is used to relate the activation enthalpy $\Delta E + P\Delta V$ in expression (1) to melting temperature:

$$\frac{\Delta E + P\Delta V}{\mathrm{k}} = g\,T_{melt}$$

The utility of using expression (2) is that knowledge of the pressure-dependence of activation energy and activation volume, which is difficult to measure directly at high pressures, can be replaced by pressure-dependent melting temperature. The latter can be measured at moderate pressures and extrapolated to high pressures (*i.e.*, the deep mantle). For olivine, g values between 20 and 30 have been suggested, depending on whether diffusion or dislocation creep are assumed (*e.g.*, *Weertman & Weertman*, 1975).

Understanding the long time scale rheology of the mantle as represented by its effective viscosity, is a central and enduring problem in global geophysics. The diverse methods and data sets which have been employed to constrain mantle viscosity have been a source of ongoing contention and debate. The importance and intensity of this debate are a reflection of the fundamental role of mantle viscosity in controlling a wide array of geodynamic processes. For example, millennial time scale glacial isostatic adjustment (GIA) processes such as Pleistocene and Holocene sea-level variations and related anomalies in Earth's gravitational field and rotational state are known to be strongly dependent on the depth dependence of mantle viscosity. On much longer, million to hundred-million year time scales, viscosity exerts fundamental control on the dynamics of mantle convection and on the corresponding evolution of the thermal and chemical state of Earth's interior. The very long time scale implications of mantle viscosity also include fundamental surface geological and geophysical processes, such as global scale epeirogeny and associated sea level changes, global geoid anomalies and tectonic plate motions.

The first and most influential geophysical contribution to our understanding of mantle viscosity is Haskell's (1935) study of Fennoscandian post-glacial uplift which was found to require an average viscosity of 10^{21} Pa s down to a depth approximately equal to the horizontal dimension of the surface load (about 1000 to 1500 km). Haskell's inference of the average value of viscosity in the top $\sim$1400 km of the mantle has turned out to be a remarkably robust estimate which has been repeatedly verified by a very large number of geodynamic studies carried out over the past 70 years.

3. Energetics of the Earth

3.1. Internal energy sources for Earth dynamics

The movements of Earth's tectonic plates and the enormous amounts of energy released by earthquakes and volcanic activity must be driven by energy sources inside our planet. The fundamental question we must consider is what are these energy sources and how is this energy transmitted to Earth's surface?

There are three main sources of energy which have been identified:

- radioactivity
- secular cooling (i.e. loss of primordial heat trapped inside the Earth)
- gravitional energy release (e.g. from growth of Earth's inner core)

Radioactivity

With the discovery of naturally occurring radiaoactive elements in crustal rocks, it was recognized that radioactive decay could be a very important source of heat in Earth's interior. From geochemical studies of the composition of the Sun and chondritic meteorites, we know that the most significant heat producing radioactive isotopes in the Earth are U^{238}, U^{235}, Th^{232}, K^{40}. The heat generated by the decay of these elements is given by the expression

$$Q_{rad} = [U] \; \left(Q_U + \frac{[Th]}{[U]} Q_{Th} + \frac{[K]}{[U]} Q_K \right)$$

in which $[U]$, $[Th]$, $[K]$ are the concentrations of the radiaoctive elements in the solid Earth and Q_U, Q_{Th}, Q_K are the corresponding heat production rates (W/kg).

The ratios of potassium to uranium, $[K]/[U]$, and thorium to uranium, $[Th]/[U]$, are estimated from abundances in the Sun and in the carbonaceous chondrite meteorites and they are bout 10^4 and 4, respectively. (Potassium is a volatile element so it is possible that the actual ratio $[K]/[U]$ may be lower in the Earth.) If we now take the concentration of uranium measured in carbonaceous chondrites to be $[U] = 2 \times 10^{-8}$ kg/kg (i.e. 20 parts per billion), we obtain

$$Q_{rad} \approx 4.6 \times 10^{-12} \text{ W/kg}$$

which implies about 18 TeraWatts of internal radioactive heating for the whole Earth (for a mantle mass of $M \sim 4 \times 10^{24}$ kg).

Obviously, because of the radiaoctive decay, the radioactive abundances in the solid Earth today are less than in the past. It is estimated that internal radioactive heat abundance today is about a factor of two less than it was 3 billion years ago.

Secular cooling

Because the Earth had higher heat production in the past it must undergo cooling over time. This bulk cooling rate can be estimated by comparing petrologically determined geothermal gradients in Archean igneous rocks with that in present-day rocks and it is found that the bulk cooling rate is about

$$\frac{100^\circ}{\text{billion years}}$$

This cooling rate can be used to calculate the thermal energy release from the Earth's interior using the following expression:

$$Q_{sec}(t) = -M\, C_P \frac{\mathrm{d}T}{\mathrm{d}t}$$

where C_P is the specific heat capacity and M is the mass of the Earth. Using $C_P \approx 1000$ J/kg/K we then obtain

$$Q_{sec} = 15 \times 10^{12} \text{ W}$$

We note that heat loss by secular cooling is comparable in importance to radioactive heating.

Gravitational energy release

The differentiation and redistribution of matter that occurred inside the Earth after its accretion 4.5 billion years ago implies a change to a lower state of gravitational energy because heavy matter (e.g. iron) sinks towards the Earth's centre. This reduction in gravitational energy is ultimately released as heat. The most important differentiation event is the formation of Earth's metallic core. It is estimated that the descent of iron into the Earth's centre released about 10^{31} J of energy to form the core. We can estimate the change in temperature of the Earth if all the energy produced by core formation is trapped inside the Earth:

$$\Delta E = M_E \, C_P \, \Delta T$$

where $M_E \approx 6 \times 10^{24}$ kg is the mass of the Earth. From $\Delta E = 10^{31}$ J, we calculate $\Delta T \approx 3500$ K. This increase in temperature would be enough to completely melt the Earth, so it is likely that the heat released by core formation was not trapped inside the Earth but rather was radiated out into space during the accretion process.

An important source of gravitational energy release that is occuring today is associated with the growth of the solid inner core from the condensation of iron in the liquid outer core. The gravitational energy release associated with inner core growth is an important driving force for the geomagnetic dynamo and it provides a source of heat which is transmitted to the mantle at the core-mantle boundary.

3.2. Heat flow at Earth's surface

The thermal energy produced in Earth's interior must ultimately be transmitted to the Earth's surface in the form of heat flow. This heat flow exists becauses the temperature in Earth's crust increases with depth and therefore the surface heat flow q is given by Fourier's law:

$$q = -k\frac{\mathrm{d}T}{\mathrm{d}z} \tag{3}$$

where z is the depth and k is the thermal conductivity of crustal rocks. Notice the minus sign which tells us that heat always flow down to lower temperatures. In three dimensions, Fourier's law of heat conduction is written as

$$\boldsymbol{q} = -k\boldsymbol{\nabla}T \;\text{ where }\; \boldsymbol{\nabla} = \left(\frac{\partial}{\partial \mathrm{x}}, \frac{\partial}{\partial \mathrm{y}}, \frac{\partial}{\partial \mathrm{z}}\right) \tag{4}$$

In Earth's crust the dominant variation of temperature is with depth and hence it is sufficient to use expression (3) to model the surface heat flow.

Surface heat flow measurements have been conducted on a global scale, both on land and also on the sea floor. The results of these global measurements are summarized in the map below.

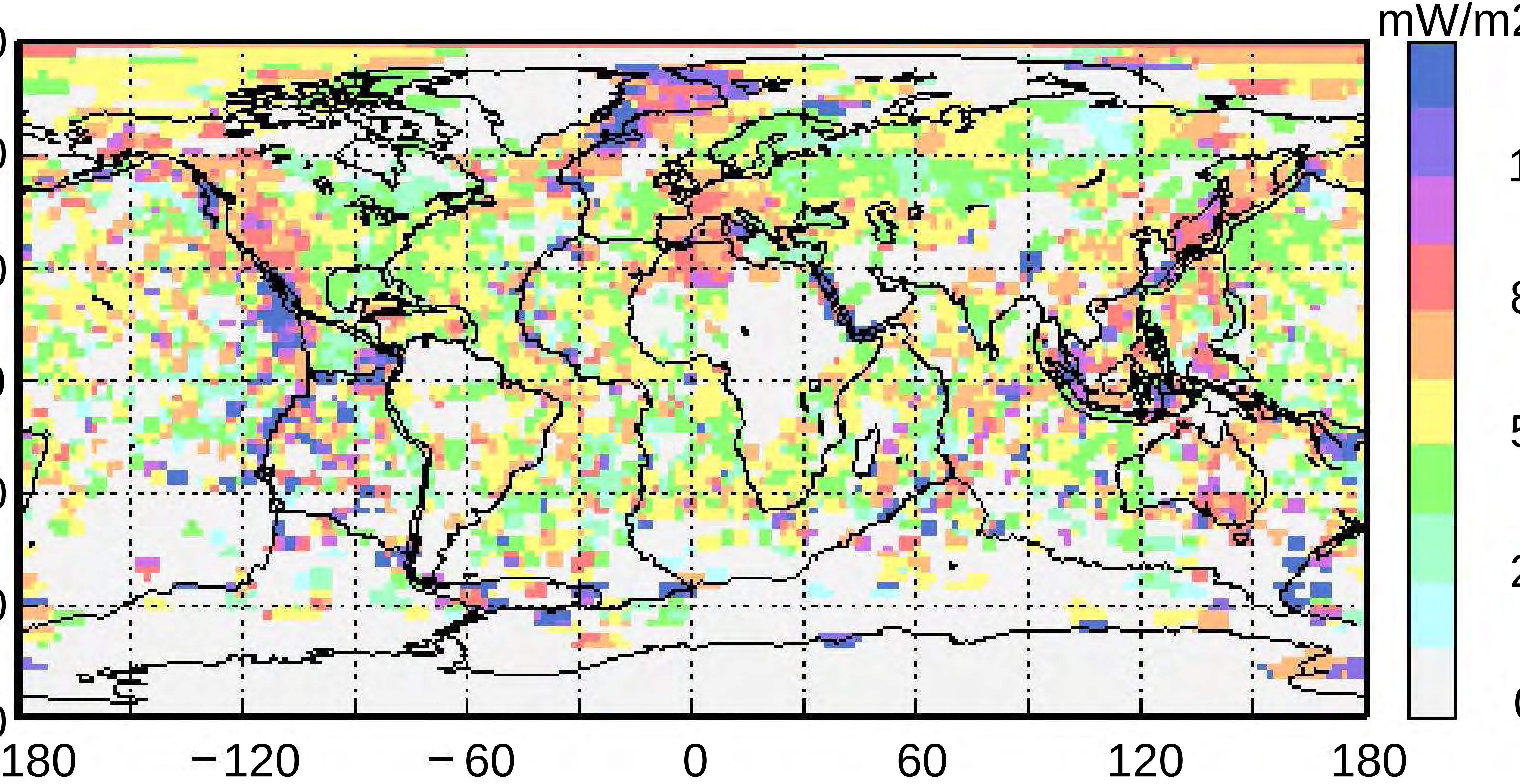

Measured surface heat flow (uncorrected for hydrothermal circulation)

A summary of these heat flow measurements, distributed according to the age of the rocks in each of the measurement sites, is tabulated below.

Mean Heat Flow Values

Description	Mean Heat Flow, mW m^{-2} Observed	Stein and Stein, [1992]	Age Range, Ma	
		Oceanic		
Cenozoic undifferentiated	89.3	125.2	0.0	66.4
Mesozoic undifferentiated	44.6	51.0	66.4	245.0
Quaternary	*139.5**	*806.4**	0.0	1.6
Pliocene	*109.1**	*286.0**	1.6	5.3
Miocene	*81.9**	*142.2**	5.3	23.7
Oligocene	*62.3**	*93.4**	23.7	36.6
Eocene	*61.7**	*75.7**	36.6	57.8
Paleocene	*65.1**	*65.1**	57.8	66.4
Late Cretaceous	61.5	60.0	66.4	84.0
Middle Cretaceous	56.3	53.9	84.0	119.0
Early Cretaceous	53.0	50.5	119.0	144.0
Late Jurassic	51.3	49.4	144.0	163.0
		Continental		
Subaqueous continental undifferentiated	77.7			
Cenozoic sedimentary and metamorphic	63.9			
Cenozoic igneous	97.0			
Mesozoic sedimentary and metamorphic	63.7			
Mesozoic igneous	64.2			
Paleozoic sedimentary and metamorphic	61.0			
Paleozoic igneous	57.7			
Proterozoic	58.3			
Archean	51.5			

Mean Oceanic Heat Flow = 101 mW/m^2

Mean Continental Heat Flow = 65 mW/m^2

Mean Global Heat Flow = 87 mW/m^2

Total Global Heat Loss = 44 TW

The rocks of the continental crust are significantly more enriched in radioactive heat producing elements that the oceanic crustal rocks. Geochemical and petrological models of the abundance of heat producing elements in the continental crust suggest that as much as 8 TW of heat production are concentrated in the continental crust. Since the total thermal power loss at the Earth's surface is 44 TW (see table above), we estimate that 36 TW of heat flow comes from the mantle.

3.3. Mechanisms of heat loss

The three principal mechanisms for heat transfer are radiation, conduction and convection, where the last two are the most important in the solid Earth. Heat transfer by conduction was described above and it is given by Fourier's law (see equation 4).

Heat transfer by convection involves the material transport of thermal energy as illustrated schematically in the diagram below:

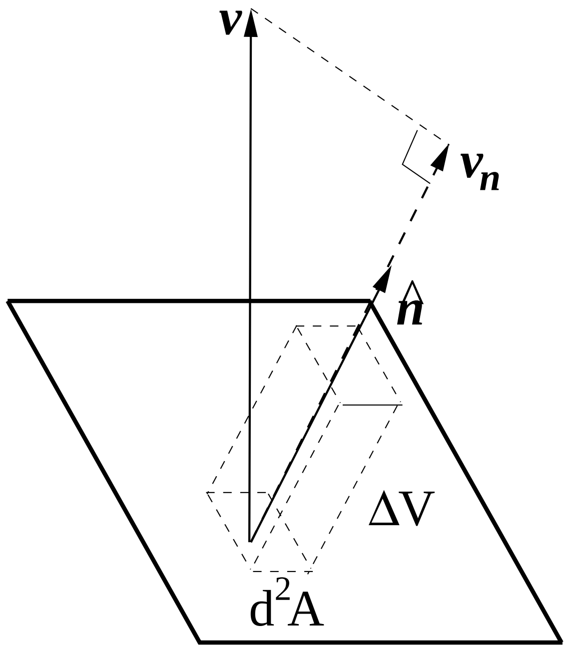

In a small interval of time δt, the quantity of mass transported perpendicular to the surface d^2A, in the direction of the unit normal vector $\hat{\boldsymbol{n}}$, is given by:

$$\rho\,(\Delta V) = \rho\,(d^2A\; v_n \delta t) = \rho\, \boldsymbol{v}\cdot\hat{\boldsymbol{n}}\,(d^2A\;\delta t)$$

From this expression we find that the mass flux vector (mass transport per unit area per unit time) is given by

$$\text{mass flux} = \rho\, \boldsymbol{v}\cdot\hat{\boldsymbol{n}} \tag{5}$$

We can now use expression (5) to find the thermal energy flux (heat energy per unit area per unit time) due to mass transport using $\Delta E = \Delta M \, C_P \, T$,

$$\text{convective heat flux} = \rho \, C_P \, T \, \boldsymbol{v}\cdot\hat{\boldsymbol{n}} \quad (\text{units: W/m}^2) \tag{6}$$

Which heat transfer mechanism, conduction or convection, is important inside the Earth? To answer this question we will first consider the principle of energy conservation in order to have a quantitative understanding of how temperature changes inside the Earth.

3.4. Conservation of energy in the mantle

To derive the temperature equation from the principle of energy conservation we will first consider a simplified treatment of a 1-D thin slab geometry shown below:

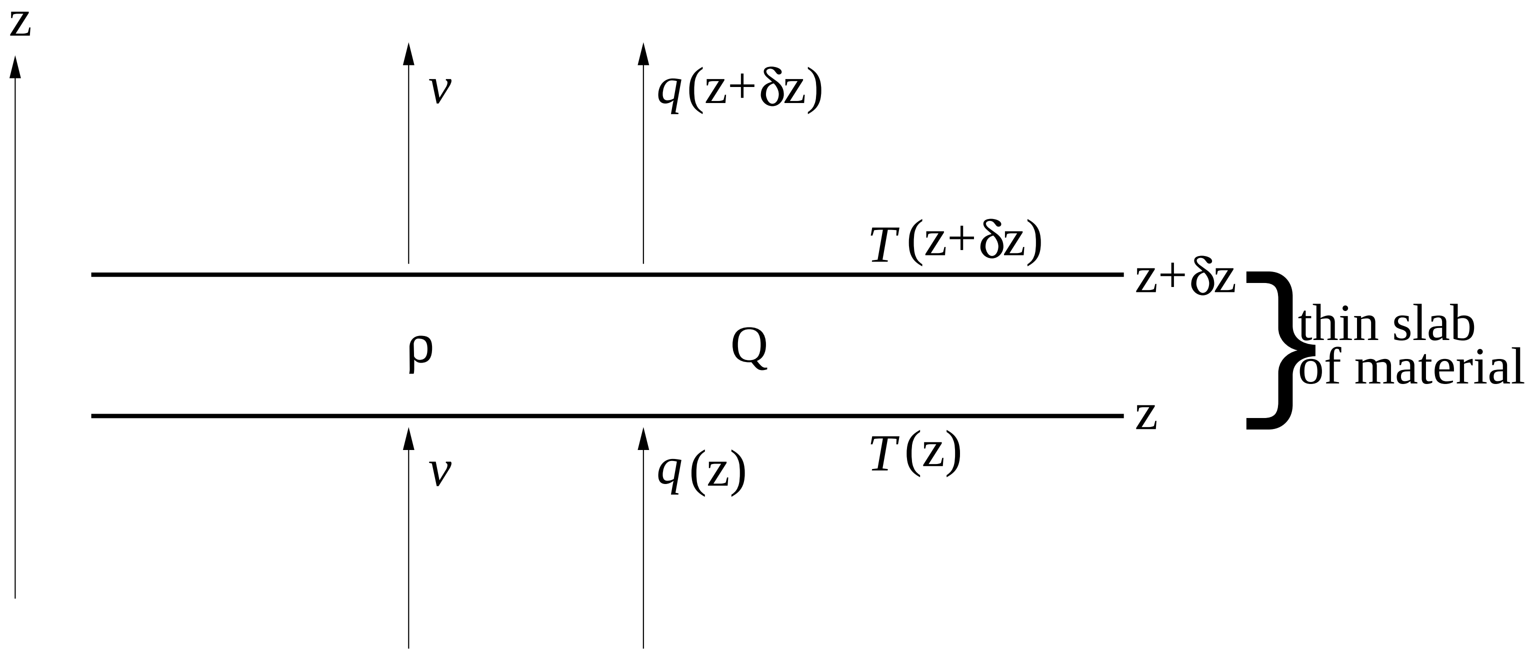

in which v is the flow velocity, q is the conductive heat flux, Q is the radioactive heat generation per unit mass, and ρ is the mass density.

From the expression $\Delta E = M\ C_P\ \Delta T$, the time rate of change of thermal energy of the slab per unit area is given by the expression

$$\frac{\partial E}{\partial t} = \rho\, \delta z\, C_P\ \frac{\partial T}{\partial t} \tag{7}$$

The rate of internal heat production per unit area is given by

$$Q \, \rho \, \delta z \tag{8}$$

The total rate of heat loss from thermal conduction is

$$\begin{aligned} q(z+\delta z) - q(z) &= \frac{\partial q}{\partial z} \, \delta z \\ &= -k \frac{\partial^2 T}{\partial z^2} \, \delta z \end{aligned} \tag{9}$$

in which we have used Fourier's law: $q = -k \partial T / \partial z$.

The rate of convective heat loss is determined using expression (6) above:

$$\rho \, C_P \; v \, T(z+\delta z) - \rho \, C_P \; v \, T(z) = \rho \, C_P \; v \; \frac{\partial T}{\partial z} \, \delta z \tag{10}$$

Notice here that we have assumed that the density ρ is constant (does not change with position z).

The principle of conservation of energy applied to the thin slab is as follows:

$$\begin{aligned} \text{rate of change of energy (7)} = &\quad \text{rate of internal heat production (8)} \\ - &\quad \text{heat loss by conduction (9)} \\ - &\quad \text{heat loss by convection (10)} \end{aligned}$$

If we now substitute expression (7–10) into this energy conservation law we obtain (after some simple rearrangement of terms):

$$\rho\, C_P \left[\frac{\partial T}{\partial t} + v\, \frac{\partial T}{\partial z} \right] = k\, \frac{\partial^2 T}{\partial z^2} + \rho\, Q \qquad (11)$$

We can similarly show that in 3-D, the principle of energy conservation for an incompressible (i.e. constant density) material is

$$\boxed{\frac{\partial T}{\partial t} + \boldsymbol{v} \cdot \boldsymbol{\nabla} T = \kappa \nabla^2 T + \frac{Q}{C_P} \qquad (12)}$$

in which $\kappa = k/(\rho\, C_P)$ is called the thermal diffusivity.

To understand the relative importance of conductive and convective heat transfer in the mantle let us introduce characteristic scales for length L and velocity v. If we non-dimensionalize the temperature equation (12) using these scales we obtain:

$$\frac{\partial T}{\partial t} = -\frac{v}{L}\boldsymbol{v'}\cdot\boldsymbol{\nabla'}T + \frac{\kappa}{L^2}\nabla'^2 T + \frac{Q}{C_P} \tag{13}$$

From this equation we immediately see that the convection and conduction time scales are, respectively,

$$t_{conv} = \frac{L}{v} \quad t_{cond} = \frac{L^2}{\kappa}$$

The ratio of these two time scales is called the Peclet number:

$$Pe = \frac{t_{cond}}{t_{conv}} = \frac{Lv}{\kappa}$$

If we use values appropriate for the mantle: $L = 3 \times 10^6$ m (depth of the mantle), $v = 4 \times 10^{-2}$ m/yr (mean velocity of tectonic plates), $\kappa \approx 10^{-6}$ m^2/s, we obtain $Pe \approx 3600$. We thus find that conductive time scales are more than 3 orders of magnitude larger than convective time scales and this implies that the most efficient heat transport mechanism in the mantle is convection.

4. Quantitative Modelling of Mantle Convection Dynamics

It is now clear that in order to understand the dynamics of heat and mass transport in Earth's interior we must develop models of thermal convection in the mantle which, we hope, are sufficiently realistic. There are now three basic approaches we can take in developing these models: (1) numerical computer-based simulations, (2) flow modelling based on seismic tomographic images of mantle structure, and (3) controlled fluid mechanical experiments in a laboratory.

The first approach is by far the most popular and it has a long history, dating back to the classical work of *McKenzie et al.* [1974]:

J. Fluid Mech. (1974), vol. 62, part 3, pp. 465–538

Convection in the earth's mantle: towards a numerical simulation

By D. P. McKENZIE, J. M. ROBERTS
Department of Geodesy and Geophysics, University of Cambridge

AND N. O. WEISS
Department of Applied Mathematics and Theoretical Physics, University of Cambridge

Plate tectonics provides a remarkably accurate kinematic description of the motion of the earth's crust but a fully dynamical theory requires an understanding of convection in the mantle.

This paper established a path which has been followed by a large number of subsequent numerical studies which are far too numerous to cite here.

The basic governing principles used by *McKenzie et al.* [1974] to numerically model mantle convection are:

- conservation of mass
- conservation of momentum (Newton's 2nd law: F = ma)
- conservation of energy

The resolution of these conservation laws requires the following supplementary equations which are specific to the mantle:

- dependence of stress on strain rate (constitutive relation)
- an equation of state which expresses the dependence of density on temperature and pressure (and perhaps on chemical composition)

We have already derived the conservation of energy equation for an incompressible mantle (see equation 12). In the following we will also derive expressions for the conservation of mass and momentum.

4.1. Conservation of mass

To derive the mass conservation equation we will again consider a simplified treatment of a 1-D thin slab geometry shown below:

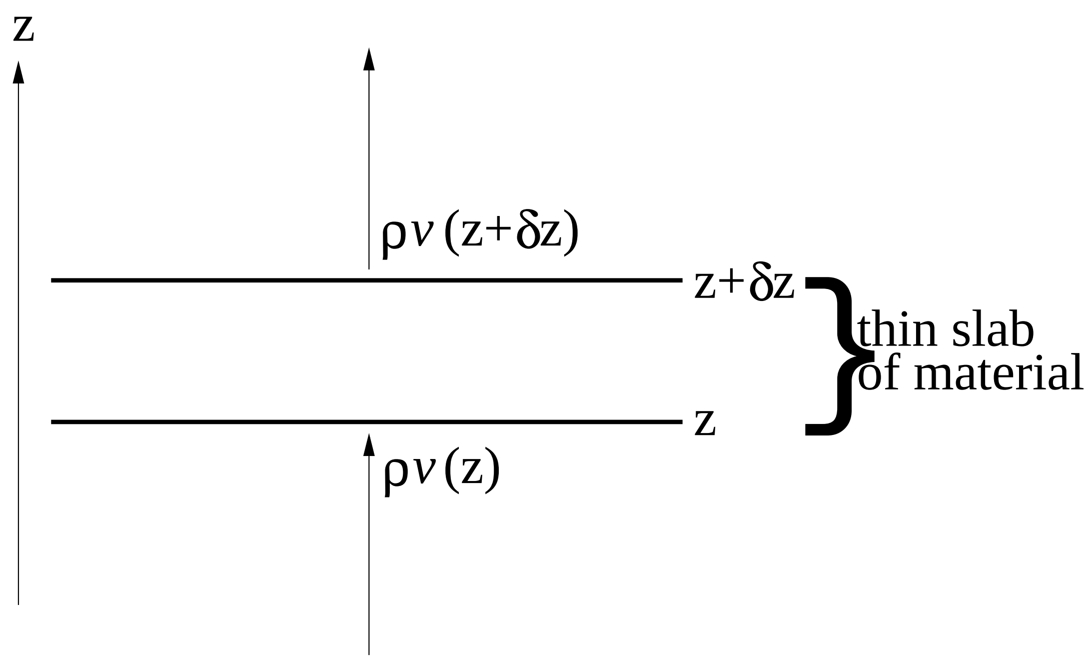

in which ρv is the mass flux (mass/unit area/unit time) which was introduced above in expression (5)

From the expression $\Delta M = V \Delta \rho$, where V is the volume occuppied by the mass M, the time rate of change of the mass of the slab per unit area is given by the expression

$$\frac{\partial M}{\partial t} = \delta z \, \frac{\partial \rho}{\partial t} \tag{14}$$

The rate of mass loss by the mass flux out of the slab is:

$$\rho v(z + \delta z) - \rho v(z) = \frac{\partial(\rho v)}{\partial z}\, \delta z \tag{15}$$

The principle of mass conservation applied to the thin slab is as follows:

rate of change of mass (14) $=$ $-$mass loss by flow (15)

If we now substitute expression (14, 15) into this conservation law we obtain:

$$\frac{\partial \rho}{\partial t} + \frac{\partial(\rho v)}{\partial z} = 0 \tag{16}$$

We can similarly show that in 3-D, the principle of mass conservation material is

$$\boxed{\frac{\partial \rho}{\partial t} + \boldsymbol{\nabla}\cdot(\rho \boldsymbol{v}) = 0 \qquad (17)}$$

If we assume an incompressible mantle (density is constant), the mass conservation equation (17) reduces to the following simple expression:

$$\boldsymbol{\nabla} \cdot \boldsymbol{v} = 0 \tag{18}$$

4.2. Conservation of momentum

One can show that the application of Newton's 2nd law of mechanics (the principle of momentum conservation) to a continuous mass distribution yields the following very general equation valid in any abitrary 3-D coordinate system:

$$\rho \frac{\mathrm{d}\boldsymbol{v}}{\mathrm{dt}} = \boldsymbol{\nabla} \cdot \boldsymbol{\sigma} + \rho \mathbf{g} \tag{19}$$

in which $\boldsymbol{v}$ is the velocity field, $\boldsymbol{\sigma}$ the stress tensor, $\mathbf{g}$ the gravitational acceleration and ρ the density.

The stress tensor $\boldsymbol{\sigma}$ describes the mutual contact forces acting across any surface inside the Earth and it is therefore one of the most important physical quantities in Earth dynamics.

In a Cartesian coordinate sytem the stress tensor may be represented by a 3×3

symmetric matrix:

$$\boldsymbol{\sigma} \rightarrow \begin{pmatrix} \sigma_{xx} & \sigma_{xy} & \sigma_{xz} \\ \sigma_{xy} & \sigma_{yy} & \sigma_{yz} \\ \sigma_{xz} & \sigma_{yz} & \sigma_{zz} \end{pmatrix} \tag{20}$$

In the case of a incompressible fluid medium with a characteristic viscosity η, the stress tensor is given by the following expression:

$$\sigma_{ij} = -P\delta_{ij} + \eta \left(\frac{\partial v_i}{\partial x_j} + \frac{\partial v_j}{\partial x_i} \right) \tag{21}$$

where δ_{ij} is the identity tensor, P is the total pressure, and $\partial v_i / \partial x_j$ represents the derivative of the velocity component v_i with respect to the coordinate direction x_j.

If we now subsitute the viscous stress tensor (21) into the momentum equation (19) we obtain the famous Navier-Stokes equation of fluid mechanics:

$$\eta \nabla^2 \boldsymbol{v} - \boldsymbol{\nabla} P + \rho \mathbf{g} = \rho \frac{\mathrm{d}\boldsymbol{v}}{\mathrm{dt}} \tag{22}$$

in which we have assumed that the viscosity η is a constant.

Before we proceed further, it will be instructive to consider a nondimensional version of the fluid momentum conservation equation. We will employ the following scale variables

$$(x, y, z) = (d\,x', d\,y', d\,z')$$
$$t = t_{cond}\,t' \quad \text{where} \quad t_{cond} = (d^2/\kappa)$$

where the original variables are on the left and the non-dimensional ones are on the right and indicated with primes. The length scale d is arbitrary and κ is the thermal diffusivity. On the basis of these length and time scales we can further non-dimensional velocity v, pressure P and body force ρg as follows:

$$\boldsymbol{v} = d/t_{cond}\,\boldsymbol{v'}, \quad P = \eta/t_{cond}\,P', \quad \rho\mathbf{g} = \eta/(d\,t_{cond})\,\rho'\mathbf{g}'$$

If we finally substitute all these non-dimensionalized quantities into the fluid dynamical equation (22) we obtain:

$$\nabla'^2 \boldsymbol{v'} - \boldsymbol{\nabla'} P' + \rho' \mathbf{g}' = \frac{1}{Pr} \frac{\mathrm{d}\boldsymbol{v'}}{\mathrm{dt}'} \tag{23}$$

in which

$$Pr = \frac{t_{cond}}{t_{visc}}, \quad \text{where} \quad t_{visc} = \rho d^2/\eta$$

is called the Prandtl number which characterises the ratio of temperature and momentum diffusion time scales. In the case of the Earth's mantle we estimate that $t_{visc} = 3 \times 10^{-5}$ s and $t_{cond} = 6 \times 10^{18}$ s, thus yielding

$$Pr = 2 \times 10^{23}$$

The very high value for the Prandtl number in the mantle means that all inertial (acceleration) forces are completely insignificant and hence the Navier-Stokes equation reduces to:

$$\eta \nabla^2 \boldsymbol{v} - \boldsymbol{\nabla} P + \rho \mathbf{g} = 0 \tag{24}$$

The infinite Prandtly number approximation for the mantle implies there must at all times be a balance between the buoyancy forces $\rho\mathbf{g}$ and the forces of viscous disspation described by $\eta\nabla^2\boldsymbol{v}$. In other words, any changes in internal buoyancy forces will instantly produce changes in mantle flow.

In the absence of convection in the mantle, when $\boldsymbol{v} = 0$, the equation of motion (24) reduces to:

$$-\boldsymbol{\nabla} P_o + \rho_o \mathbf{g} = 0 \tag{25}$$

in which P_o, ρ_o, are the pressure, density in the hydrostatic state. This equation describes an idealized *equilibrium reference state* for the mantle.

If we subtract the hydrostatic reference state (25) from the equation of motion (24), we finally obtain the perturbed equation of motion which describes mantle flow dynamics:

$$\eta\nabla^2\boldsymbol{v} - \boldsymbol{\nabla}(\delta P) + (\delta\rho)\mathbf{g} = 0 \tag{26}$$

In a convecting mantle the density perturbations $\delta\rho$ are produced by temperature anomalies in the mantle. We can determine the thermally induced density perturbations from the equation of state $\rho = \rho(P, T)$ and therefore

$$\delta\rho = \left(\frac{\partial\rho}{\partial T}\right)\delta T = -\alpha\rho\delta T$$

where α is the coefficent of thermal expansion. Therefore the equation of motion which is appropriate for a convecting mantle is:

$$\eta \nabla^2 \boldsymbol{v} - \boldsymbol{\nabla}(\delta P) = \alpha \rho \mathbf{g} \delta T \tag{27}$$

4.3. Numerical simulations of mantle convection

We may finally assemble all the equations we derived for the numerical simulation of thermal convection dynamics in an incompressible mantle (density assumed constant, except for thermal expansion):

• conservation of mass

$$\boldsymbol{\nabla} \cdot \boldsymbol{v} = 0$$

• conservation of momentum

$$\eta \nabla^2 \boldsymbol{v} - \boldsymbol{\nabla}(\delta P) = \alpha \rho \mathbf{g} \delta T$$

• conservation of energy

$$\frac{\partial T}{\partial t} + \boldsymbol{v} \cdot \boldsymbol{\nabla} T = \kappa \nabla^2 T + \frac{Q}{C_P}$$

The first large scale computational simulations of mantle convection in simple 2-D Cartesian geometry by *McKenzie et al.* [1974] demonstrated the feasability for carrying out detailed numerical investigations into the tranport of heat and mass in Earth's mantle and to better understand the thermal evolution of our planet.

In spite of the significant computational difficulties in obtaining 'realistic' numerical simulations of mantle convection in a fully 3-D spherical geometry, there has been encouraging progress over the past few years, as is illustrated in the following figure:

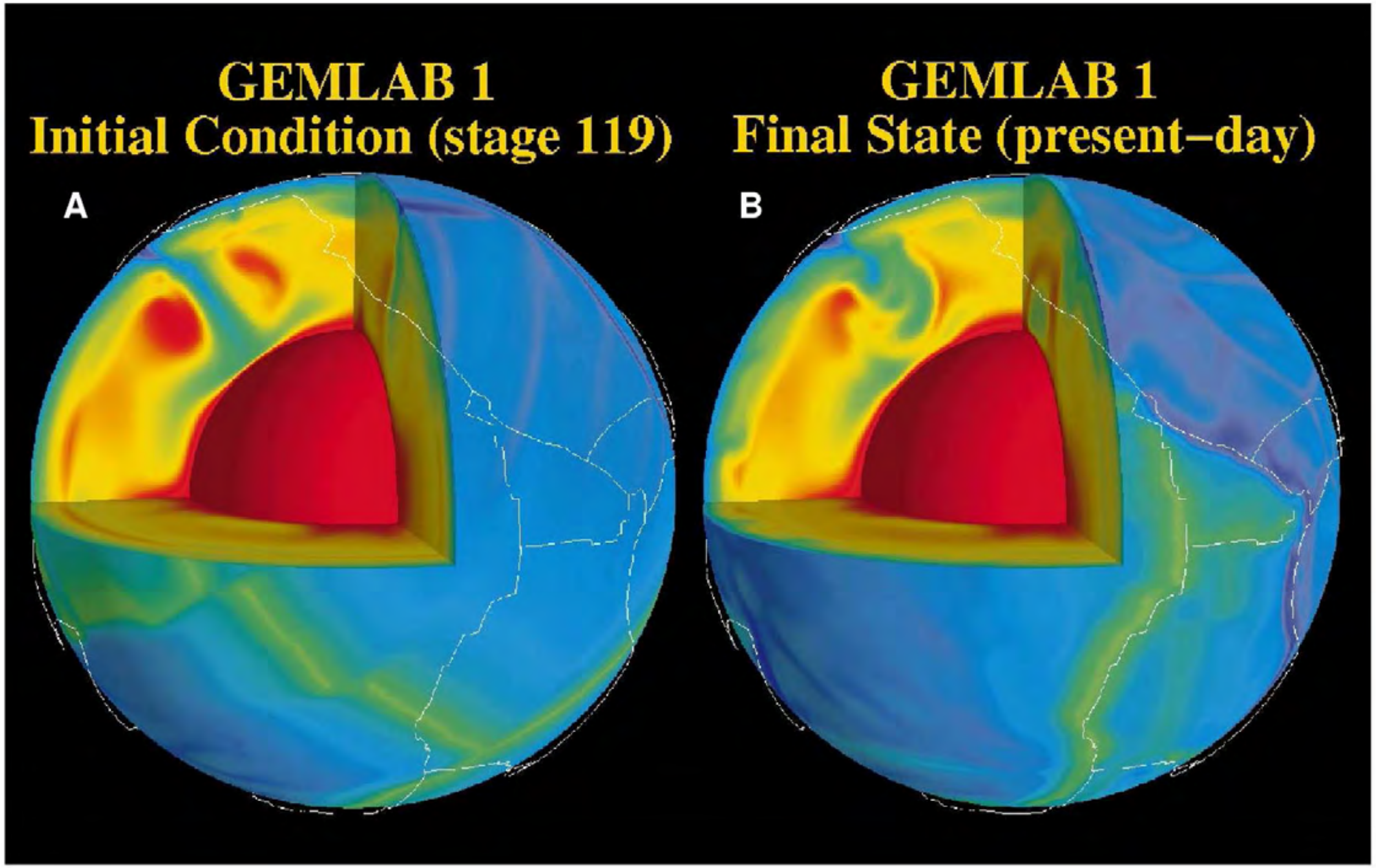

Fig. 2. Numerical convection simulation incorporating time-dependent plate-tectonics (from *Bunge et al.* [1998])

4.4. Mantle convection and global seismic tomography

The time-dependent convection simulation in Fig. 2, shows a dynamical regime which is almost completely dominated by cold descending plumes which correspond to subducted slab heterogeneity. This dominance arises from the assumption of strong internal heating, which is compensated by cooling from above, and it is characterized by the absence of active hot plumes ascending from the CMB.

The convection simulation in Fig. 2 predicts a pattern of thermal heterogeneity which appears to be quite different from that revealed by global *seismic tomographic imaging*. Global tomography models have consistently revealed the presence of major plume-like structures in the deep mantle. The presence of such deep-seated plumes is clearly apparent in Fig. 3 which shows the S-wave heterogeneity in the tomography model *SH12_WM13* of *Su et al.* [1994].

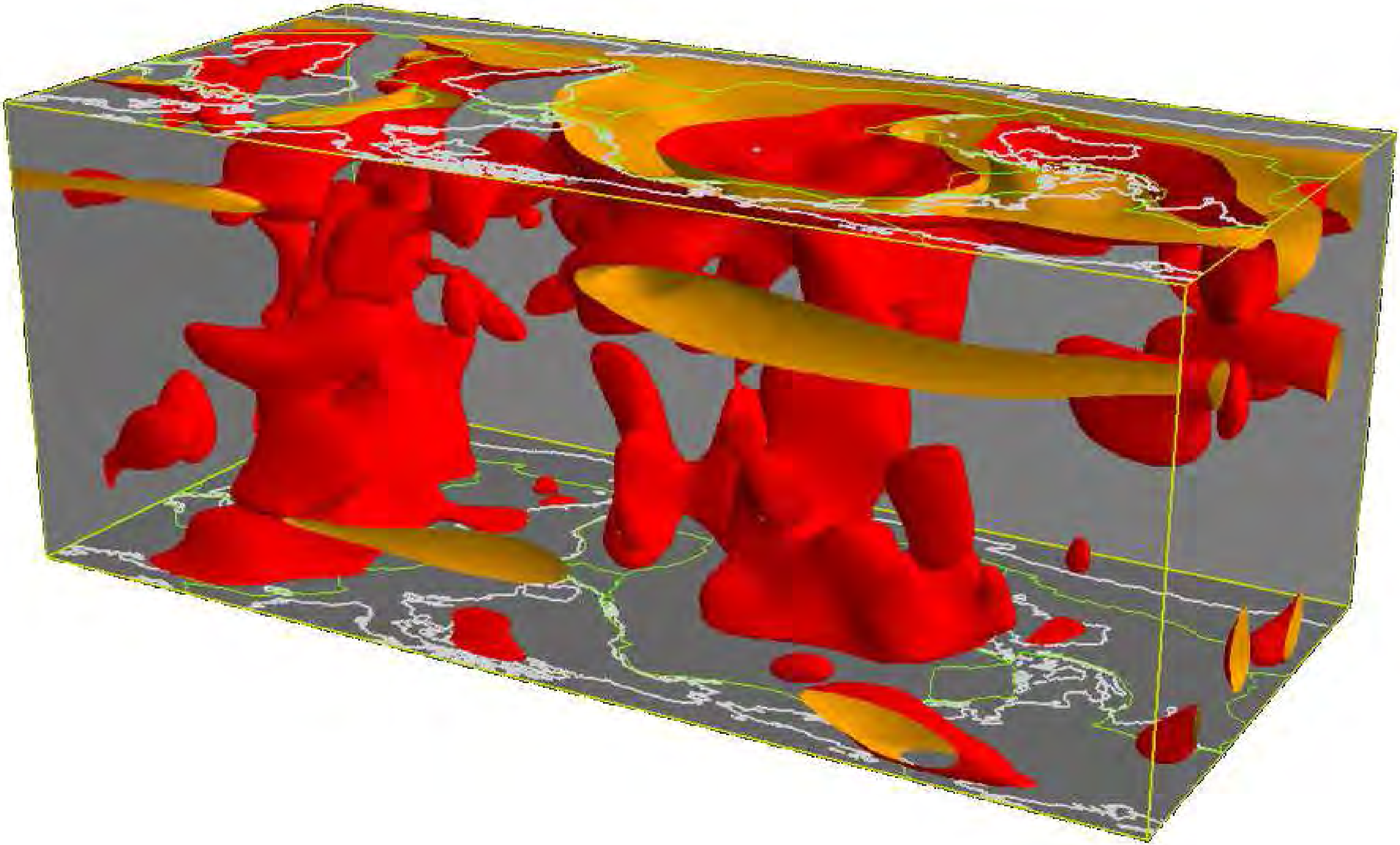

Fig. 3. Mantle heterogeneity (from *Su et al.* [1994]) for all regions in which $\delta Vs/Vs < -0.6\%$.

The significant discrepancies between the recent numerical convection simulations (e.g., Fig. 2) and the seismic tomographic images (e.g., Fig. 3) are a reminder of the progress which must still be made before the purely numerical convection simulation can properly explain the structure and evolution of 3-D mantle structure. These difficulties suggest a *second approach for modelling mantle dynamics*, namely to use the mantle structure revealed by the tomography models as a proxy for the thermal anomalies which are maintained by the thermal convection process in the mantle.

> This tomography-based modelling of the mantle convective flow is equivalent to assuming that the conservation of energy equation has already been 'solved' (at least for the present-day temperature anomalies) by global seismic tomographic imaging.

In the following we will carry out a detailed development of this alternative approach to the study of convection dynamics in the mantle. We will therefore focus on models which can predict the 3-D buoyancy-induced flow corresponding to seismically imaged mantle heterogeneity. We will apply these flow models to explore the relationship between seismically inferred 3-D mantle structure and the various surface manifestations of convection dynamics.

With this alternative approach to modelling mantle dynamics we can fully exploit the detailed heterogeneity revealed by the most recent global tomography models, as in the following figure.

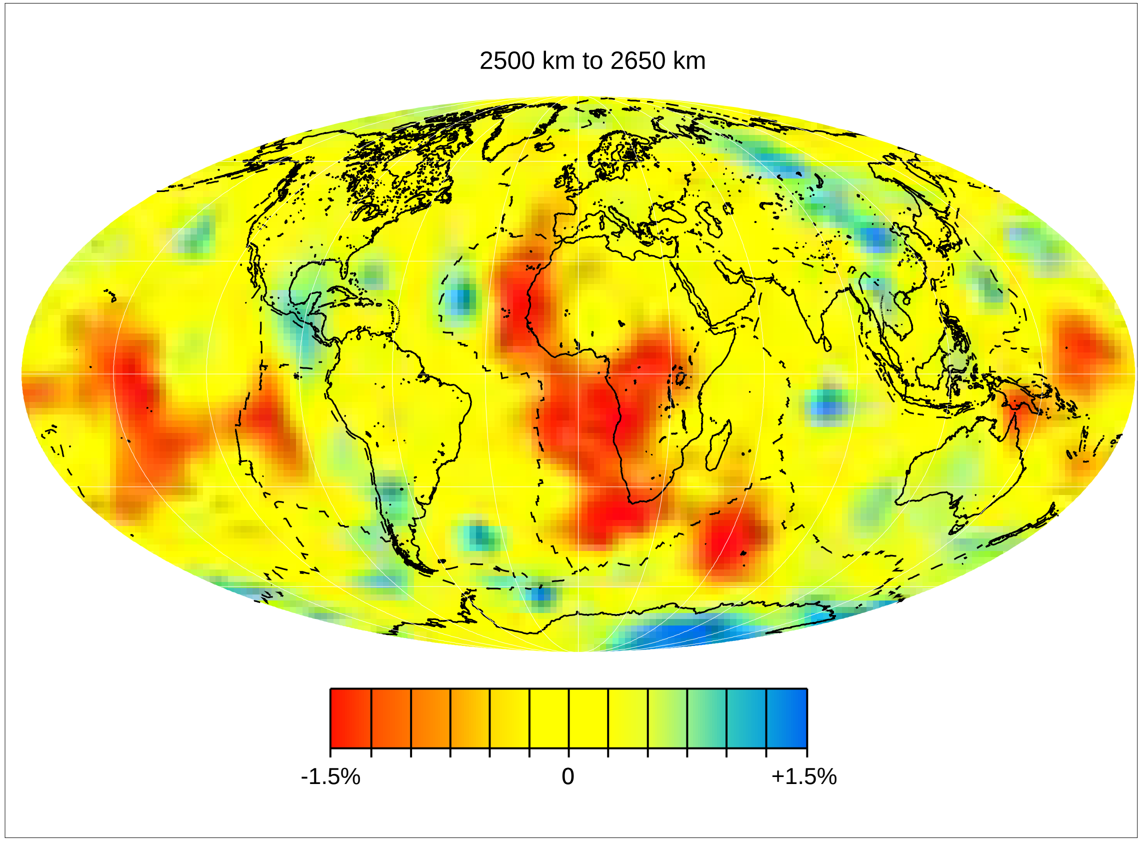

Fig. 4. Lower-mantle S-wave heterogeneity [*Grand*, 2002].

4. References

- Akimoto, S., and H. Fujisawa, Olivine–spinel solid solution equilibrium in the system Mg_2SiO_4–Fe_2SiO_4, *J. Geophys. Res.*, **73**, 1467–1479, 1968.
- Backus, G, A class of self-sustaining dissipative spherical dynamos, *Ann. Phys.*, **4**, 372–447, 1958.
- Boschi, L., and A.M. Dziewonski, Whole Earth tomography from delay times of *P*, *PcP*, and *PKP* phases: Lateral heterogeneities in the outer core or radial anisotropy in the mantle? *J. Geophys. Res.*, **105**, 13,675–13,696, 2000.
- Bunge, H.-P., M.A. Richards, C. Lithgow-Bertelloni, J.R. Baumgardner, S.P. Grand, and B.A. Romanowicz, Time scales and heterogeneous structure in geodynamic Earth models, *Science*, **280**, 91–95, 1998.
- Constable, S.C., R.L. Parker, and C.G. Constable, Occam's inversion: A practical algorithm for generating smooth models from electromagnetic sounding data, *Geophys.*, **52**, 289–300, 1987.
- Corrieu, V., C. Thoraval, and Y. Ricard, Mantle dynamics and geoid Green functions, *Geophys. J. Int.*, **120**, 516–523, 1995.
- Defraigne, P., Internal loading of a compressible Earth: Effect of a solid lithosphere *Phys. Earth Planet. Inter.*, **101**, 303–313, 1997.
- De Mets, C.R., R.G. Gordon, D.F. Argus, and S. Stein, Current plate motions, *Geophys. J. Int.*, **101**, 425–478, 1990.
- Dziewonski, A.M., and D.L. Anderson, Preliminary reference Earth model, *Phys. Earth Planet. Inter.*,

25, 297–356, 1981.

- Forte, A.M., and W.R. Peltier, Plate tectonics and aspherical Earth structure: The importance of poloidal–toroidal coupling, *J. Geophys. Res.*, **92**, 3645–3679, 1987.
- Forte, A.M., and W.R. Peltier, Viscous flow models of global geophysical observables,1 Forward problems *J. Geophys. Res.*, **96**, 20,131–20,159, 1991.
- Forte, A.M., and J.X. Mitrovica, New inferences of mantle viscosity from joint inversion of long-wavelength mantle convection and post–glacial rebound data, *Geophys. Res. Lett.*, **23**, 1147–1150, 1996.
- Forte, A.M., and H.K.C. Perry, Geodynamic evidence for a chemically depleted continental tectosphere, *Science*, **290**, 1940–1944, 2000.
- Forte, A.M., and J.X. Mitrovica, Deep-mantle high-viscosity flow and thermochemical structure inferred from seismic and geodynamic data, *Nature*, **410**, 1049–1056, 2001.
- Forte, A.M., W.R. Peltier, and A.M. Dziewonski, Inferences of mantle viscosity from tectonic plate velocities, *Geophys. Res. Lett.*, **18**, 1747–1750, 1991.
- Grand, S.P., Mantle shear-wave tomography and the fate of subducted slabs, *Phil. Trans. R. Soc. Lond. A*, **360**, 2475–2491, 2002.
- Hager, B. H., Subducted slabs and the geoid: Constraints on mantle rheology and flow, *J. Geophys. Res.*, **89**, 6003–6015, 1984.
- Hager, B.H., and R.W. Clayton, Constraints on the structure of mantle convection using seismic

observations, flow models, and the geoid, in *Mantle Convection: Plate tectonics and global dynamics*, edited by W. R. Peltier, pp. 657–763, Gordon and Breach (New York), 1989.

- Haskell, N.A., The motion of a viscous fluid under a surface load, *Physics* (N.Y.), **6**, 265–269, 1935.
- Jackson, J.D., *Classical Electrodynamics*, John Wiley (New York), 1975.
- Karato, S., and B.B. Karki, Origin of lateral variation of seismic wave velocities and density in the deep mantle, *J. Geophys. Res.*, **106**, 21,771–21,784, 2001.
- King, S.D., Models of mantle viscosity, in *A Handbook of Physical Constants: Mineral Physics and Crystallography*, edited by T.J. Ahrens, pp. 227–236 AGU Reference Shelf Series, vol. 2, American Geophysical Union (Washington DC), 1995.
- Landau, L.D., and E.M. Lifshitz, *Fluid Mechanics*, vol.**6**, Pergamon (New York), 1959.
- Liu, L., The post–spinel phase of forsterite, *Nature*, **262**, 770–772, 1976.
- Marsh, J.G., et al., The GEM–T2 gravitational model, *J. Geophys. Res.*, **95**, 22043–22071, 1990.
- Mathews, P.M., T.A. Herring, and B.A. Buffett, Modeling of nutation and precession: New nutation series for nonrigid Earth and insights into the Earth's interior, *J. Geophys. Res.*, **107**(B4), 2068, doi:10.1029/2001JB000390, 2002.
- McKenzie, D.P., J.M. Roberts, and N.O. Weiss, Convection in the Earth's mantle: Towards a numerical simulation, *J. Fluid Mech.*, **62**, 465–538, 1974.
- Mitrovica, J.X., Haskell[1935] revisited, *J. Geophys. Res.*, **101**, 555-569, 1996.

- Mitrovica, J.X., and A.M. Forte, Radial profile of mantle viscosity: Results from the joint inversion of convection and postglacial rebound observables, *J. Geophys. Res.*, **102**, 2751–2769, 1997.
- Panasyuk, SV., B.H. Hager, and A.M. Forte, Understanding the effects of mantle compressibility on geoid kernels, *Geophys. J. Int.*, **124**, 121–133, 1996.
- Parsons, B., and S. Daly, The relationship between surface topography, gravity anomalies, and the temperature structure of convection, *J. Geophys. Res.*, **88**, 1129–1144, 1983.
- Pekeris, C.L., Thermal convection in the interior of the Earth, *Mon. Not. R. Astron. Soc.*, *Geophys. Suppl.* **3**, 343–367, 1935.
- Phinney, R.A., and R. Burridge, Representation of the elastic-gravitational excitation of a spherical Earth model by generalized spherical harmonics, *Geophys. J. R. Astron. Soc.*, **34**, 451–487, 1973.
- Ranalli, G., and B. Fischer, Diffusion creep, dislocation creep, and mantle rheology, *Earth Planet. Sci. Lett.*, **34**, 77–84, 1984.
- Ricard, Y., L. Fleitout, and C. Froidevaux, Geoid heights and lithospheric stresses for a dynamic Earth, *Ann. Geophys.*, **2**, 267–286, 1984.
- Richards, M.A., and B.H. Hager, Geoid anomalies in a dynamic Earth, *J. Geophys. Res.*, **89**, 5987–6002, 1984.
- Ringwood, A.E. Phase transformations and mantle dynamics, *Earth Planet. Sci. Lett.*, **14**, 233–241, 1972.
- Ringwood, A.E., and A. Major, Synthesis of Mg_2SiO_4–Fe_2SiO_4 spinel solid solutions, *Earth Planet. Sci. Lett.*, **1**, 241–245, 1966.

- Sammis, C.G., J.C. Smith, G. Schubert, and D.A. Yuen, Viscosity-depth profile of the Earth's mantle: Effects of polymorphic phase transitions, *J. Geophys. Res.*, **82**, 3747–3761, 1977.
- Su, W.–J., R.L. Woodward, and A.M. Dziewonski, Degree 12 model of shear velocity heterogeneity in the mantle, *J. Geophys. Res.*, **99**, 6945–6980, 1994.